ADAPTIVE IMPEDANCE CONTROLLER FOR PROSTHETIC HAND OBJECT GRASPING AND MANIPULATION

A Thesis by

Jose D. Esquivel-Ortiz

Bachelor of Science in Biomedical Engineering, Wichita State University, 2016

Submitted to the Department of Mechanical Engineering
and the faculty of the Graduate School of
Wichita State University
in partial fulfillment of
the requirements for the degree of
Master of Science

May 2021

OBJECT GRASPING ADAPTIVE IMPEDANCE CONTROLLER IMPLEMENTATION FOR UPPER EXTREMITY PROSTHETIC

The following faculty members have examined the final copy of this thesis for form and content and recommend that it be accepted in partial fulfillment of the requirement for the degree of Master of Science, with a major in Mechanical Engineering.

_____

Yimesker Yihun, Committee Chair

_____

Hamid Lankarani, Committee Member

_____

Jaydip Desai, Committee Member

DEDICATION

To my wonderful wife who continuously pushes me to become a better man, together with her life is worthwhile.

ACKNOWLEDGEMENTS

I would like to say thank you to Dr. Yimesker Yihun, not only for the guidance and information he has provided me as a professor and mentor but for also having the patients to always continue working with me. It is difficult to work full time in your career and try to complete a graduate program. Especially one as challenging as the Wichita State Mechanical Engineering Department where they strive for excellence. As I was completing my graduate degree, I have never had one negative experience. Every class I took was challenging; however, I am grateful for how much I have learned. The knowledge I have required in the subject of robotics and control systems will be incredibly useful for my career continuation in the industry

In addition, I would like to acknowledge my wife for the support she provided me during this process. Finishing my thesis would have been much more difficult without her. Also, I would like to thank my family for their support. At a young age my mother pushed me to get my education. It was difficult at times since she was a single mother, and I did not have the support of two parents, but I never let that hold me back. With the support of my wife, family, and the Mechanical Engineering department I was able to fulfill one of my lifelong dreams.

ABSTRACT

There are many complexities involving the human hand's ability to perform stable grasping patterns. Human grasping is a complicated function to mimic in relation to prosthetic hands. Although there are various state-of-the-art-prosthetic mechanisms currently in the market that can perform different types of grasping patterns; these mechanisms still lack the ability to determine specific grasping stability properties. To improve prosthetic hand grasping, impedance control can be utilized. Impedance control provides the ability to adjust the dynamic relations between the robotic movements and the exterior forces in a continuous manner. In this study an impedance control algorithm is developed.

The proposed impedance control algorithm will deal with uncertainties including object friction, physical properties, and contact points. The software known as SynGrasp will be utilized to model a hand to object grasping configuration. In addition, the scenario where an object is being perturbed while being grasped will be performed and analyzed. By utilizing grasping configuration properties, a grasp stability estimator function will determine if the final grasp (after the object is perturbed) is more stable or not. Quality measures for the initial grasp and final grasp will be calculated and analyzed. The data will then be used to determine if the stabilizing algorithm is needed or not. SynGrasp will also be used to provide all the data needed for the impedance stabilizing algorithm. The stability estimation function is the most crucial component in the impedance control algorithm. By utilizing SynGrasp a successful estimation function for an impedance control algorithm was created and tested. By incorporating this impedance control system to a prosthetic hand mechanism. The prosthesis will be one step closer in mimicking the dexterity of a human hand.

TABLE OF CONTENTS

TABLE OF CONTENTS (continued)

LIST OF TABLES

Table Page

LIST OF FIGURES

LIST OF ABBREVIATIONS

PI2	Policy Improvement with Path Integrals
RL	Reinforcement Learning
DOF	Degree of Freedom
VIAs	Variable Impedance Actuators
VF	Virtual Frame
PID	Proportional Integral Derivative
GUI	Graphical User Interface
DH	Denavit-Hartenberg

LIST OF SYMBOLS

$f_{f,i}$	Fingertip Contact Forces
H	Inertial Frame
f_{ext}	External Perturbation Force
M_0	Inertia Matrix
$\ddot{x}$	Vector x
p_o	Position of The Object Frame Origin
p_i	Position of the Contact Points on the i-th Finger
G	Grasping Matrix
J	Jacobean Hand Matrix
K	Stiffness
F_N	Normal Force
x_{1_c}	Contact Position
x_1	Initial Position
$f_{f,gi}$	Grasping Force
K_{gi}	Grasping Stiffness
L_i	Desired Distance Between the i-th Fingertip and the Object Frame Origin
{B}	Localization of Frame
{N}	Workspace/Wrist Frame
n_c	Total Amount of Contact Wrenches Exerted on A Ridged Body
i	Finger Contact Points
m	Map
k	Grasping Fingers
ψ_{ci}	Finger Map
M	Configuration Manifold
T_m	Tangent Space At m
R^3	Rigid Body With 3 Position Frames

$\omega_{i,hnd}^{N}$	Angular Velocity
$\upsilon_{i,hnd}^{N}$	Translation Velocity
Z_i	Plücker Coordinates Matrix
$\hat{\mathrm{z}}_j$	z-Axis Unit Vector
ζ_j	Coordinate Frame Origin Relating to j-th Joint
$\nu_{i,hnd}$	Partial Hand Jacobean
GG^T	Eigenvalues
$\sigma_{min}(G)$	Singular Configuration Quality Measure
$\sigma_{min}\ (H)$	Distance to Singular Configuration Quality Measure
T	Finger Joint Torques
$\dot{\theta}$	Velocities
v	Velocities
Q_{VME}	Singular Values of H Quality Measurement
$\Delta\sigma$	Soft Synergy Variations
Δz_r	Synergy Reference Variation Values
k_d	Desired Stiffness
$J_{f,i}^{T}$	Finger Jacobean
$\tau_{f,i}$	Finger Torque
k_f	Final Stiffness
e	Error

CHAPTER 1

INTRODUCTION

1.1 Background and Motivation

The human hand can perform very delicate tasks as it has a greater dexterity and flexibility. Loss of hand function is a serious issue as it can significantly affect the patient's ability to perform daily tasks and significantly reduce the patient's quality of life. Loss of hand function can be caused due to several reasons, such as, stroke, traumatic injury etc. According to a study done by Armour, B.S., et al, it is estimated that 1.7% of the United States population is living with some form of paralysis [1]. Paralysis is caused by problems in the spinal cord; more specifically, it is when the ability to move or control the body is lost below the point of the spinal cord where the synapse connection is affected. When the synapse connection is disconnected, communication within the nervous systems is reduced. 33.7% of those with paralysis were due to stroke while 27.3% was due to spinal cord injury, 18.6 was due to Multiple Sclerosis, and 8.3% was due to cerebral palsy. Two thirds of those living with paralysis in the US are between the ages of 18 and 65 years, 51.7% of them being women, further emphasizing that paralysis can affect anyone. Upper limb amputation can also cause loss of hand functions. In the US alone it is estimated that 185,000 people lose an upper limb through amputation a year [2]. Reasons for upper limb amputations include trauma, diabetes, bone/joint cancer, and dysvascular disease.

To combat hand function loss due to paralysis or limb amputation, prosthetic mechanisms have been created. Prosthetic hands have been primarily designed for grasping task [3]. These tasks require a high level of dexterity, sensing, complex interfaces, and advanced control systems [4, 5]. There has been significant research done in prosthetic hands that have created some sophisticated mechanisms; however, there are still some requirements that are not being met. One

reason is the lack of smooth communication between the human and the mechanism [6], as well as the limitation of the mechanical designs and control systems in mimicking the human hand dexterity. Control system algorithms can be designed in order to combat some of these issues. By designing a more efficient estimation function which focuses on defining the stability of grasp patterns, a more efficient control algorithm can be developed which can eventually be applied to prosthetic hands. This will not only improve the science of prosthetic engineering, but also allow the opportunity to create mechanisms that are one step closer to mimicking the dexterity of the human hand. Thus, allowing the return of some form of upper limb function to those who have lost it due to paralysis or amputation.

1.2 Research Objective

There are many complexities involving the human hand's ability to perform stable grasping patterns. Human grasping is a complicated function to mimic in relation to prosthetic hands. Although there are various state-of-the-art prosthetic mechanisms currently in the market that can perform different types of grasping patterns; these mechanisms still lack the ability to determine specific grasping stability properties. The objective of this thesis is to introduce an adaptive impedance control algorithm which will utilize impedance control properties as an alternative way to create and maintain stability while grasping. This research aims to develop an impedance control method that will define a stability standard for a prosthetic hand when grasping an item. In addition, the impedance control method will provide the prosthetic hand the ability to re-stabilize if the grasping stability is disrupted by perturbation being applied to the item being grasped. The MATLAB extension program known as SynGrasp was utilized to analyze the proposed algorithm.

1.3 Organization of the Thesis

This thesis is structured in the following order:

- Chapter 1 presents background, motivation, and research objectives. It provides a brief introduction about the causes of paralysis/amputation and statistics on who is affect in the US. This chapter also includes an introduction to prosthetic hands. Including what the shortcoming to prosthetic mechanisms are as well as describing how prosthetic hands can help those suffering from paralysis and amputation.
- Chapter 2 presents the literature review of the existing current prosthetic and available in the Market. In addition, the relationship between stiffness, force, and impedance controllers is reviewed. This chapter also discusses the current impedance control method studies in robotics and how impedance control can improve grasping.
- Chapter 3 presents the robust grasping impedance controller processes. In specific each section of the control algorithm will be reviewed, and the inner components will be explained.
- Chapter 4 presents the implementation of the proposed control systems using a MATLAB tool known as SynGrasp. It is discussed how SynGrasp can be used to define each component needed to complete the proposed control algorithm previously described in chapter 3.
- Chapter 5 presents a SynGrasp Study where the proposed impedance control system is performed. The study compares the differences in grasping configurations and provided data in relation grasping study. In addition, this chapter discussed potential future work.
- Chapter 6 concludes with the feasibility of design in terms of application, its advantages, limitations, and suggestions for future works.

CHAPTER 2

LITERATURE REVIEW

2.1 Current Prosthetic Hands Available in the Market

To combat upper limb amputations, state-of-the-art prosthetic mechanisms have been introduced into the market. These prosthetic mechanisms can be utilized to return grasping functionality to patients who have lost the ability. An example of a state-of-the-art prosthetic hand that is currently available in the market is the Bebionic hand (Figure 1). By utilizing myoelectric technology the user has the ability to adduct the prosthetic hand finger's which can be utilized to perform grasping tasks and patterns [7]. By adding the ability to differentiate between two different thumb positions, this allows the Bebionic to have the ability in performing 14 different grasping patterns. Examples of these grasping patterns include key grip, pinch grip, mouse grip, power grip, etc .

Figure 1: Bebionic Hand [7]

Another example of a state-of-the-art prosthetic upper limb available in the market for purchase is the i-Limb Ultra Figure 2. Similar to the Bebionic, the i-Limb Ultra utilizes myoelectric technology in specific muscle signals which is utilized to control the prosthetic limb to perform a specific task [8]. By utilizing individually motorized digits in the thumb, the i-Limb Ultra can perform 18 different gripping patterns which can be utilized for grasping tasks. In addition to the i-Limb Ultra, the company Touch Bionics also has a more advanced prosthetic hand version known as the i-Limb Quantum (Figure 3). With the use of gesture control this prosthetic mechanism is capable of performing 36 different grip patterns available.

Figure 2: i-Limb Ultra hand [8]

Figure 3: i-Limb Quantum Hand [8]

3D printing is revolutionizing prototyping and is being used in many medical applications which included prosthetic mechanisms [9]. For example, The Hero Arm produced by Open Bionics is the first medically certified 3D printed prosthetic hand Figure 4. Although aesthetically the Hero Arm is more superior to models like the Bebionic and the i-Limb, it does lack the ability to perform the various gripping patterns. Although the described prosthetic hand mechanisms are considered state-of-the-art technology, they all lack the ability to determine if the grasping patterns they are producing are stable or not. Although these advanced mechanisms can perform grasping patterns and possess slip detection, they lack stability definition. When these mechanisms perform grasping patterns, in some cases using force control, there is nothing defining the stability of the overall grasp with the relationship of the object. In addition, if the object is being perturbed and the stability of the grasp is affected, these mechanisms lack the ability to properly determine if re-stabilizing is needed based on a grasp quality measure. Although some of these mechanisms can detect slippage which can lead to an increase of force there is no real method to determine mathematically if the grasps are sable or not. By creating this method, a more advanced grasping process can be achieved improving prosthetic hand accuracy.

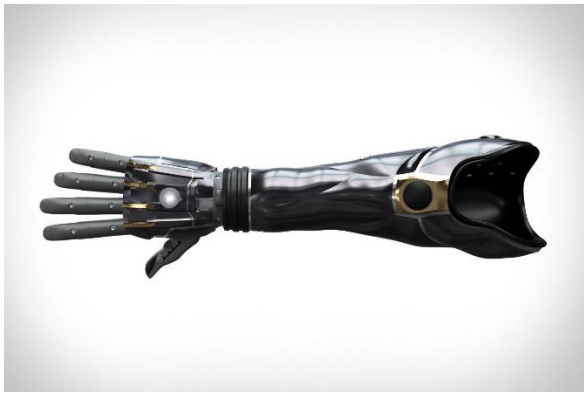

Figure 4: Hero-Arm Bionic Prosthesis Hand [9]

2.2 Relationship Between Stiffness, Force, and Impedance Controllers

Stiffness is an important factor when designing a mechanical system to perform grasping tasks [10]. Stiffness is a mechanical system property where small compliant displacements are being created while the mechanical system is sustaining loads. Quantitatively, stiffness is described as the ratio between the steady force acting on the body and the resulting compliant displacement [11-14]. Stiffness, in addition to force control, can be utilized to successfully control robotic mechanisms. Force impedance control methods can be utilized to not only control robotic mechanisms, but also ensure that the task being performed is stable. Impedance control has become a common control method for robotic mechanisms; however, these types of control methods are not commonly utilized in human controlled prosthetic limbs. By allowing the human to possess the ability to control its grasping task stability using impedance control a more human-like prosthetic limb can be developed. For example, when the human hand is holding an object and perturbations are produced on the object the human hand can adapt and ensure that its grasp on the object is stable. If combined with force control, this ability can significantly improve the quality of current prosthetic hands grasping ability.

Traditionally force control can be divided into two groups' hybrid position/force control and impedance control. Impedance control is an effective method used to improve the performance of robotic manipulations [15]. In specific, when performing an object manipulation task which includes uncertain pose estimates, physical contact, and unforeseen perturbations impedance can be utilized [16]. There are many benefits in utilizing impedance or variable impedance control; for example, impedance control allows the controlling of the dynamic relationship between the robotic movements and the external forces being produced. In addition, impedance control provides the ability to adjust the dynamic relations between the robotic movements and the exterior forces in a

continuous manner. Recently, many researchers have been using variable impedance control methods for robotic manipulations.

2.3 Current Impedance Control Methods

In the article by Buchli, J., et al, the researches perform a variable impedance control method which includes contributing a reinforcement learning algorithm [17]. The algorithm used was referred to as PI2 (Policy Improvement with Path Integrals). PI2 is a RL (Reinforcement Learning) algorithm which is derived from the first principles of stochastic optimal control. In addition, PI2 does scale to complex robotic systems. By utilizing the PI2 algorithm the researchers can optimize both trajectories while using variable impedance control. The researchers tested this method by controlling a robot known as the Phantom Premium 1.2 3-DOF Robot. PI2 allowed a greater applicability regarding optimal control with parameterized policies involving model free scenarios. In addition, mathematically the PI2 made it suitable to simultaneously optimize the reference trajectories and gain schedules. The system overview can be seen in Figure 5 where after initialization the trajectories that are planned gain schedules of the dynamic movement primitive . This dynamic movement primitive is optimized in regard to the cost function with the PI2 learning algorithm.

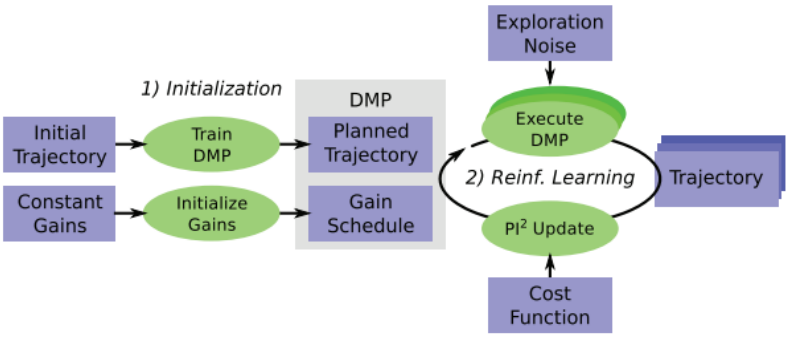

Figure 5: Reinforcement Learning Algorithm PI2 System Overview [17]

In the article Calinon, S., et al, variable impedance was utilized as a robotic control system [18]. In specific, the researchers refer to kinematic redundancies of the robot-like articles [19, 20]. A performed task which can be completed by utilizing an infinite amount of solutions is referred to as a task redundancy [21]. These redundancies are utilized to regulate the dynamics of the movement which also involves regulating the stiffness of the robot during task reproduction. By observing a similar task many times, the robot creates a model of the skill. This model considers the variations and correlations seen during the performed movement. If parts were consistent during the performed movement, then that part of the task should be reproduced. From this information the robot will set an adaptive stiffness matrix which is compatible with the task requirement. The desired task is learned by providing multiple demonstrations of the desired skill and examples of these demonstrations can be seen in Figure 6, where the experimental set up is shown for a tray handling and ironing task. Once the task constraints are extracted the robot replicates the task by selecting a variable level of compliance which will be utilized to reproduce the characteristics of the desired skill. Ultimately, the redundancies of the robot and desired tasks are exploited with the end goal of determining a safety control strategy.

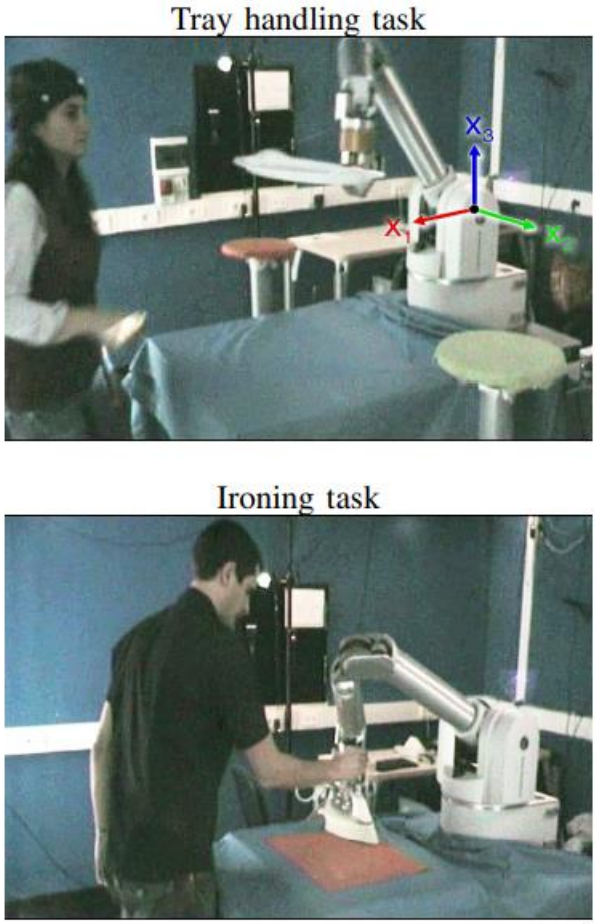

Figure 6: Redundancy Experimental Set-up [18]

In the article by K. Kronander and A. Billard, an incremental algorithm for learning variable stiffness was introduced [22]. An important component of the algorithm sets the stiffness inversely proportional to the different perturbation data created by a human subject. This article introduces a control method similar to the articles by Rozo, L., et al, and Kormushev, P., et al [23, 24], in which the robot is implicitly taught forces needed to counteract any perturbations. Normal approaches utilize interfaces provided by a teacher creating demonstration data. The demonstration data can be collected by using the robot's own body and sensors while demonstrating. This can be

done via a process known as teleoperation which consists of motion control, force control, and impedance control. The control method overview can be seen in Figure 7, where the stiffness is taught by observing the position differences in relations to the teacher interactions and the desired reference points. By allowing the robot to adapt its stiffness online the teacher gains direct haptic feedback of the teachers own interaction.

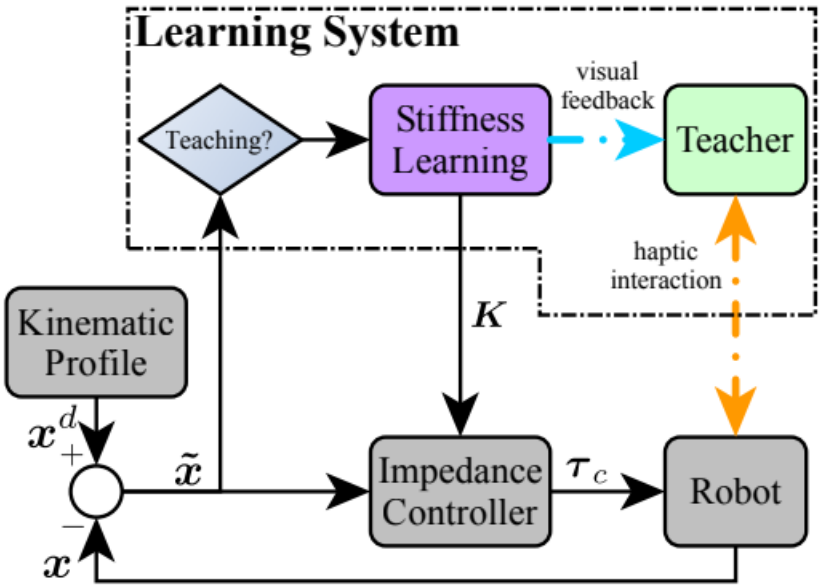

Figure 7: Control Overview Involving Learning of Varying Stiffness [22]

2.4 Utilizing Impedance Control for Improved Grasping

Humans poses a superior ability to control their limbs through contractions of muscle pairs. In specific, humans can modulate their motions which include controlling impedance. The role of impedance for humans helps regulate stability and accuracy in regard to task readiness which has been illustrated in many papers [25-27]. Various studies have been created to study stiffness in the

human body. For example, in the article by Gomi, H. and M. Kawato an apparatus for measuring human limb stiffness was introduced to study the relationship between human arm stiffness and arm control [28]. In addition article by Burdet, E., et al, reports that humans commonly change stiffness in order to deal with an instabilities caused by interactions [29]. This type of information has led researchers to develop bio-inspired algorithms which allow robots to perform tasks in changing dynamic interactions by utilizing an learning force, impedance and trajectory [30]. There have been instances where researchers utilize variable impedance to mimic human impedance behavior. For example, in the article by Howard, M., et al, a comparative study was performed which involved different approaches utilized to control robots with variable impedance actuators (VIAs) [31]. This setup can be seen in Figure 8. where motors ($u_{motor\ 1}$ and $u_{motor\ 2}$) controlled by command systems are used to model human muscles (u_{biceps} and $u_{triceps}$).

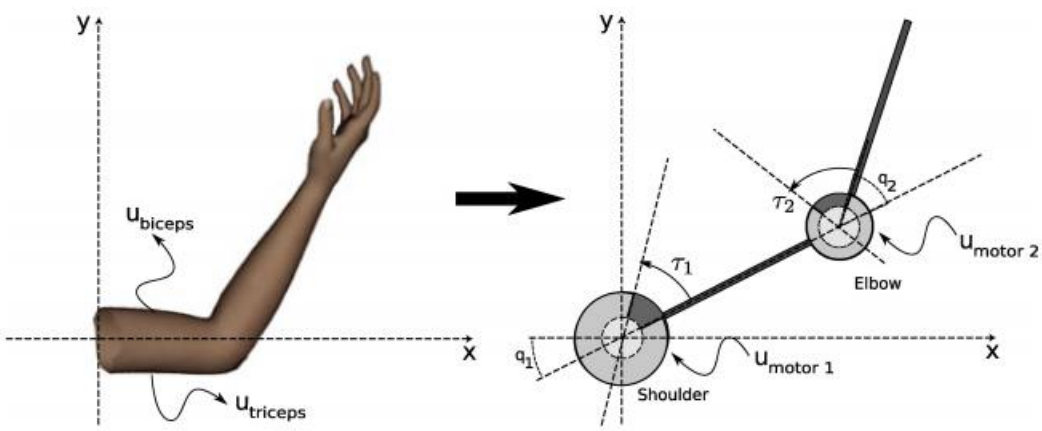

Figure 8: Actuator Modeling Used to Mimic the Human Muscles and Joints [31]

For robots to interact skillfully with their environment, like humans, force and impedance control can be utilized [29, 32]. Many applications can be implemented using impedance and force

control. For example, these applications include precision assembly task, and surgical/rehabilitation purposes [33]. Force control will provide contact stability while impedance control provides task stability against any perturbations. These tasks can include grasping. Grasping is an important task/function that at times is required for industrial application [34]. In addition, grasp performance plays a key role in successfully performing manipulation tasks [35]. Although impedance control has become a widely used robotic control method it has not been commonly utilized in human controlled prosthetic hands. When a human hand is performing a grasping task, it uses impedance properties to sustain a stable grasp when disturbances are introduced. If this ability can be mimicked and introduced to a prosthetic hand then a better-quality prosthetic can be created. In this article a force/stiffness impedance controller method is introduced. The controller will be applied to a human prosthetic limb and activated by a human signal. The impedance controller will be designed to ensure the stability is kept throughout a desired grasping motion and can re-stabilize if the grasped object is being perturbed. By incorporating an impedance control method to upper prosthetic limbs grasping stability performance will improve overall increasing the functionality of the mechanisms.

CHAPTER 3

ROBUST GRASPING IMPEDANCE CONTROL DESIGN

3.1 Robust Grasping Impedance Controller Processes

The impedance controller will consist of three components. The first component will include the initial grasp. The second component involved the stability estimation function, and the last component is known as the adaptive control component if needed. The control process algorithm flow chart can be seen in Figure 9. The impedance adaptation section will have its own control layout for further explanation.

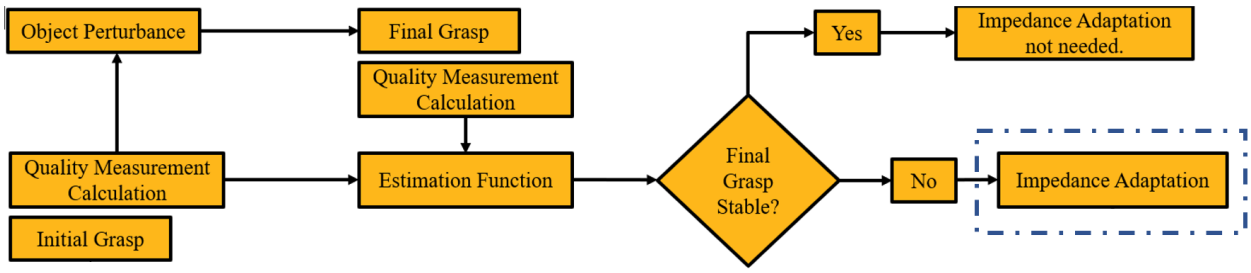

Figure 9: Control Algorithm Process Layout

3.2 Initial Grasp

The impedance controller begins with an initial grasp. This will involve the prosthetic hand's fingers creating contact positions with the objects. The object impedance and fingertip impedance can be represented as springs shown in Figure 10. Each fingertip contact position will be utilized to find the Object Virtual Frame (VF). The VF is an integral part of the proposed impedance and has been used in other control methods [36, 37]. The VF can be utilized to detect slippage regarding the object being grasped. The dynamic of the object seen Figure 10 is governed

by Equation 1 [15, 38].Where $f_{f,i} = 1,2,3$ represent the contact forces at each fingertip location being applied to the object. VF is the virtual frame or the center of the object while H is the inertial frame. f_{ext} is the external perturbation force.

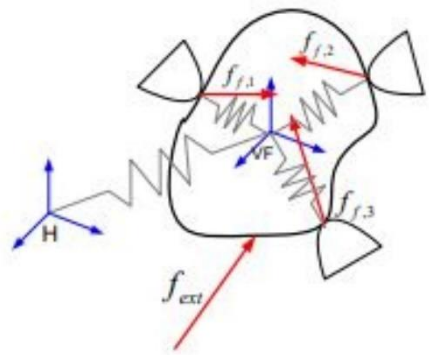

Figure 10: 3-Finger Grasping Dynamic Model [38]

$$f_{f,o} + f_{ext} = M_0\ddot{x} \tag{1}$$

3.2.1 Virtual Frame

When designing a grasp stability estimator, a concept known as Virtual Frame (VF) can be utilized to provide a position/orientation estimation of the object being grasped. A benefit of utilizing the VF concept is the fact that it is solely based on the location/position of the fingers contacting the object. Since the VF relies on finger contact location it is helpful when dealing with the many uncertainties that can be derived from the object geometry [39]. In addition, this process can reduce the number of sensors being used. The VF concept has been utilized in various articles when dealing with a 3-finger grasping pattern. For example, in the article by Li, M., et al., the origin of the VF can be found using Equation 2 [38]:

$$p_o = \frac{1}{3}\sum_{i=1}^{3} p_i \tag{2}$$

Where p_o represents the position of the object frame origin and p_i represents the position of the contact points on the i-th finger. Once the VF is defined any translation or rotational position difference between the real object and the referenced frame can be calculated. Although this three finger VF concept has been used in various papers involving grasping [37, 38], the VF method can also be calculated for hands involving more than 3 fingers [40]. The VF is an important component regarding the estimation function of the control algorithm.

3.3 Grasping Estimator

It is difficult to estimate the shape and position of an object and although methods utilizing sensory capabilities like vision have been utilized to tackle this issue, there are problems due to the lack of accuracy of vision [41, 42]. By establishing an initial grasp configuration, an estimation function can be utilized which will provide crucial information to assist in the prediction of the grasp stability. Grasp stability estimation is not a foreign concept pertaining to grasping control functions. In the article by Dang, H. and P.K. Allen, tactical sensing data is utilized to estimate grasping stability which will in return allow the ability to make the necessary hand adjustments after the estimating grasp [43]. In addition, in the article by Bekiroglu, Y., et al., utilized hepatic data and machine learning methods to create a stability estimation method [44]. The purpose of the proposed control algorithm is to create an estimation function that works with situations involving object perturbations. The proposed estimation function will utilize quality measures as determinants for stability. The grasp estimator will be utilized to predict an unstable grasp which will trigger a re-stabilization strategy.

3.4. Impedance Adaptation

The impedance adaptation component will only be necessary if the previous grasp was determined as unstable. After the initial grasp has been conducted, by utilizing the grasping matrix G and the Jacobean hand matrix J, quality measure studies can be performed on the grasping configuration. Once the initial quality measurements are conducted then the grasping configuration will be manipulated to mimic the object perturbation motion. By perturbing the object, a new hand configuration will be created. The grasp quality measurement studies will be conducted on the second grasp configuration as well. By comparing both the initial and final quality measurement data, it can be determined if the final grasp pattern (after the object is perturbed) is better or worse than the initial grasping pattern. If the final grasp is better then the configuration can be left alone; however, if the final grasp is worse then the impedance adaptation algorithm will need to be activated to stabilize the grasp. The impedance adaptation requirement layout can be seen in Figure 11.

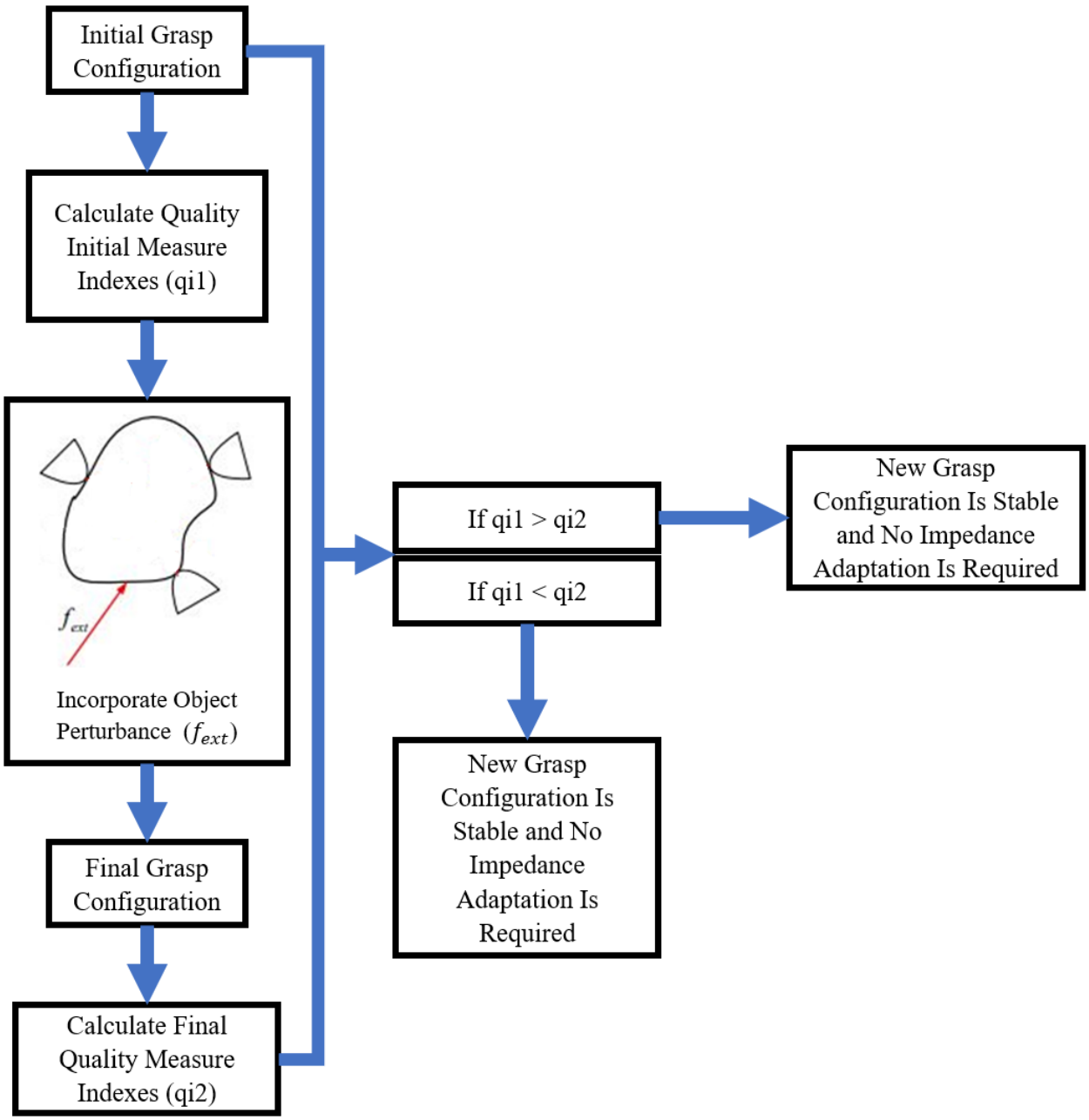

Figure 11: Impedance Adaptation Requirement Layout

3.4.1 Stable Grasping Impedance Definition

A crucial component of the grasp stability estimator function is defining what a stable grasp is. In the past, stiffness measurements focused on utilizing tactile sensors [45-47]. However, there have been many different methods used to find object stiffness that involve position and force. In

the article by Andrecioli, R. and E.D. Engeberg, the paper describes an adaptive controller which is used for position control in a powered prosthetic hand [48]. A crucial component of the control system performance is finding the object stiffness. Robotic system dynamics are very sensitive to the stiffness of the object in contact with the robot end effector because of this the object being grasped and the turning of the gains usually favor a stiff object. When a prosthetic hand is grasping different objects with different stiffnesses an adaptive control based on grasped object stiffness can be an effective improvement to the force control issues common in prosthetic mechanisms. Researchers in this article compare a PID sliding mode controller with an adaptive PID sliding mode controller. The crucial method used to determine the object stiffness involves basing the gains of the system on the stiffness K measurement. Researchers utilize the same algorithm for the object stiffness calculation which can be found in an article by Andrecioli, R. and E.D. Engeberg [49]. This algorithm involved dividing the measured normal force of the force feedback controller by difference between the position when contact with the object occurs and the initial position seen in Equation 3.

$$K = \frac{F_N}{x_{1_c} - x_1} \tag{3}$$

Like the human hand, a prosthetic hand with robust grasping capabilities should be able to comply with external perturbations from any direction. Although, providing robust grasping capabilities are limited in human prosthetic hands, grasping has been widely studied in robotics [50, 51]. Contact modeling is one of the basic subjects utilized in grasping studies. For example, in the article by Song, H., M.Y. Wang, and K, researches introduce a concept known as Contact Primitives which represents different sets of geometric surfaces that are then tested utilizing a robotic mechanism with two fingers [52]. These Contact Primitive geometric shapes are applied to the fingertips which compared to a base line flat surface shows that a more stable and robust

grasp can be produced. This article is an example of how contact surfaces can play an important role in robust grasping. The ability for the robust grasp to comply with perturbations will depend on grasp configuration and task requirement. To assist in robust grasping compliance researcher have proposed different control methods used to allow grasp stability under a wide range of uncertainties. In the article by Boutselis, G.I., et al, a methodology was proposed which involved providing task specific force closure grasps patterns [53]. The methodology was implemented to a five-finger robotic hand mechanism, factors like mechanical and geometric limitations were considered. The ability of the robotic hand to produce the correct amount of force to counter against position inaccuracies was established. A similar approach will be proposed in this article.

3.4.2 Proposed Impedance Adaptation Method

Once a grasp is considered unstable, which can be due to object perturbation, an impedance adaptation method will need to be activated to re-stabilize the grasp. For this to be successful a stable grasping impedance controller needs to be introduced which will be used to change the grasping force between the prosthetic hand fingers and the object. By changing the force between the object and the fingertips the stiffness is proportionally being affected. In addition, by changing the force between each finger while grasping the finger torques are proportionally affected creating a new hand configuration. The relationship between the finger force while grasping and the joint toques can be seen bellow [38]:

$$\tau_{f,i} = J_{f,i}^{T} f_{f,gi} \tag{4}$$

Where $\tau_{f,i}$ is the joint torque values at i-th finger. $f_{f,gi}$ is the grasping stable force at i-th finger and $J_{f,i}^{T}$ is the Jacobean at i-th finger.

In the contact model seen in Figure 10 only contact forces can be transmitted so a translational spring is used to represent the stable grasping impedance stiffness between the object's VF/center and the contact points of the fingers. The grasping forces at i-th finger that are required to change after the object is perturbed if needed for stabilization can be defined by Equation 5 which was derived from an article by Li, M., et al [38]. The grasping force i-th finger and stable grasping stiffness i-th finger is represented by $f_{f,gi}$, and K_{gi}. The position of the object VF/center and the position of the contact points are represented by the p_o and p_i while L_i represents the desired distance between the i-th fingertip and the object frame origin. If the initial grasp were more stable than the final grasp (after object perturbation) then the original grasp K_{gi} and L_i would be utilized to ensure a new stable configuration can be created. By calculating the $f_{f,gi}$ using Equation 5 the force can then be incorporated into Equation 4 with the desired finger Jacobean the new finger joint values can be calculated which will create a new stable hand configuration.

$$f_{f,gi} = K_{gi}(\|\Delta p_i\| - L_i)\frac{\Delta p_i}{\|\Delta p_i\|} \qquad (5)$$

CHAPTER 4

IMPEDANCE CONTROL IMPLEMENTATION USING SYNGRASP

4.1 SynGrasp Introduction

SynGrasp is a MATLAB function which provides tools and algorithms to assist with compliant and underactuated robotic hand research. This MATLAB tool allows the compliances like contact points in joints and transmissions in actuation systems to be model. Which aid with grasp analysis [54, 55]. There are two ways to use SynGrasp, one way is to utilize the GUI (graphical user interface) or utilize the script writing method which directly assembles and modifies the provided functions. In addition, grasping patterns can be defined using a provided planner or by directly defining contact points on the hand model fingertips. SynGrasp contains various investigative tools to analyze grasp properties which include controllable forces, object displacement, manipulation analysis, and grasp stiffness quality measures. Graphical representation and the main analysis results are provided. By utilizing SynGrasp the proposed impedance control algorithm can be implemented.

4.2 Initial Grasp Definition and Implementation

The following will define the inner components that make up the initial grasp function section of the proposed control algorithm. In order to fully define the initial grasp algorithm there are various steps that need to be implemented using SynGrasp. The first step included creating a hand model. Then applying the desired synergies or joint positions to the hand model. To define the grasp, finger contact points need to be defined and as well as the object being grasped. By utilizing the SynGrasp library this can be accomplished.

4.2.1 Hand Modeling

When defining the kinematic structure in SynGrasp, the hand is defined in terms of fingers, links, and joints. Every cell element, which is a 4 X 4 homogeneous transformation matrix in relation with the reference frame in the wrist and the reference frame defined at the beginning of each finger, contains a cell defined as *base*. A DH (Denavit-Hartenberg) table for every finger must be provided to properly define the desired hand model. More specifically a cell named *DHpars* collects a matrix with as many rows as joints in each finger and four columns, in each element. Both the *base* and *DHpars* cells contain as many elements as the number of fingers. Each row in the *DHpars* allows the definition of the joint in respects to either the preceding joint or base reference frame. Once the initial definition is complete the function *SGmakeHand()*, paired with the argument definitions provided by *SGmakeFinger()*, defines the hand structure. If needed the hand configuration can be modified using the *SGmoveHand()* function. SynGrasp has the ability to create different hand models which is beneficial when collecting grasping data. Some examples are the SGallegro, SGmidularHand, and the SGparadigmatic which can be seen in Figure 12.

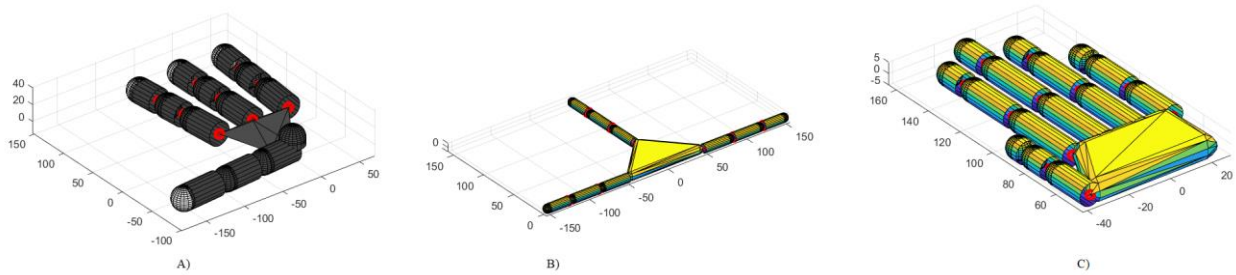

Figure 12: Hand Modeling Capability of SynGrasp.

The tools available through SynGrasp can also be utilized to study the desired hand properties involving joint displacement being coupled mechanically or by desired control algorithms. This coupling can be described as a synergy matrix which is associated with the hand model with the intent of mimicking human hand synergies [56]. The function *SGdefineSynergies()* is utilized to associate a specific hand model to the relative coupling matrix which ultimately defines a synergy matrix. *SGactivateSynergies()* activates synergies or a combination of synergies on the desired hand model [54, 55]. The movement corresponding to the initial reference configuration as well as the movement obtained by activating one or more synergies can be plotted using *SGplot – Syn()*. One of the benefits of SynGrasp is the available library. For example, the *SGparadigmatic* is an existing library function which defines a 5-fingered 20dof hand model. In addition, the *SGsantelloSynergies* library function defines the synergies for the 5-fingered 20dof hand model. The synergy matrix provided thought the function *SGsantelloSynergies* refers to data collected in the article by Santello, M., et al, which provides results suggesting that the control of hand postures involves a few postural synergies and that posture may be regulated independently from the control of the contact forces being utilized in order to grasp the desired object [57]. Figure 13 will illustrate the 5-fingered hand and Figure 14 will illustrate the hand with the desired synergies associated.

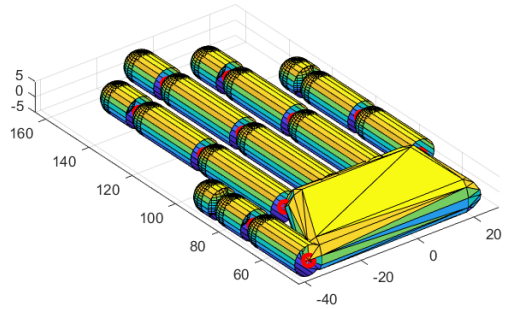

Figure 13: 5-Fingered Hand Modeled in SynGrasp

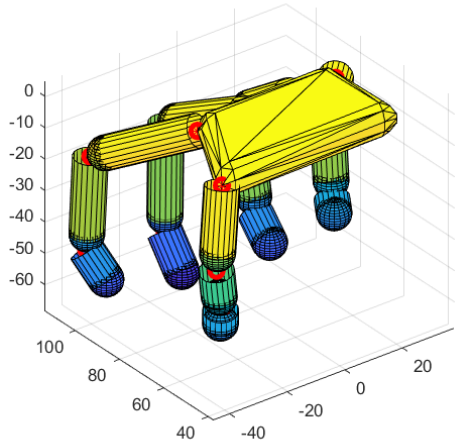

Figure 14: 5-Fingered Hand Modeled with Synergies Applied

4.2.2 Hand Grasping Definition

A crucial component of the grasping control algorithm is the relationship between the contact point locations and object definition. By utilizing a suitable contact model [58], a grasp is defined by the localization of frame *{B}* with respect to *{N}*, the contact points coordinates and the contact points respective normal forces [54, 55]. Frame *{B}* is fixed to the object frame

similar to the VF process previously described which can be seen in Figure 2. Frame {N} if fixed to the workspace/wrist frame. SynGrasp provided two ways to define these parameters. The first way is by using the function *SGaddContact(),* this function is utilized when the user wants to specify the location of the contact points. In the case where the contact points are located on the fingers, the function *SGaddFtipContact()* can be utilized. By using the function *SGmakeObject()* it is possible to create a structure representing the grasped object. By using the function *SGmakeObject()* the structural definition of the object which includes the object center, contact normal unit vectors, and the contact points can be automatically computed. SynGrasp has the ability to create different grasp models by defining different objects to grasp Figure 15. This can provide a variety of data in regard to different grasp configurations.

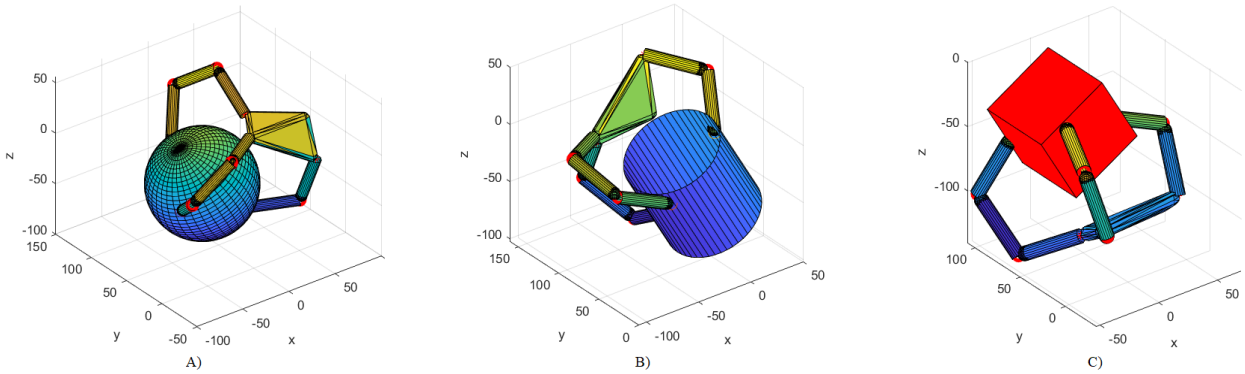

Figure 15: SynGrasp's Grasp Definition Capabilities

4.3 Stability Estimation Function Definition and Implementation Using SynGrasp

The following will define the inner components that make up the stability estimation section of the proposed control algorithm. The stability estimation function is the most crucial component of the algorithm. The need to know if the final grasp configuration after the object is perturbed is more stable or not is a crucial part of the estimation function in the proposed

algorithm. By using quality measures this can be accomplished. To calculate these quality measurements SynGrasp can utilize each grasping configuration's grasping matrix (G) and hand Jacobean (J) to calculate these indexes.

4.3.1 Defining the Grasp Matrix

After the initial grasp is defined, the quality of the grasp can be measured. Quality measure is an index that can be used to determine what a good or bad grasp is which will serve as the initial measurement starting point for determining the need for the restabilizing algorithm to be activated. Different quality measures are available which will determine the quality of a desired grasp pattern. In the article by Roa, M.A. and R. Suárez, several quality measures are reviewed and studied [59]. A benefit of SynGrasp is that the quality measures introduced in the article by Roa, M.A. and R. Suárez are also available in the SynGrasp library. In order to maximize the quality definition three quality measurement methods will be utilized. These quality measurements being used are the minimum singular value of G method, manipulability ellipsoid volume, and distance from the singular configuration.

In order to utilize these grasp quality measurements, the grasp matrix (G) and the hand Jacobean matrix (J) need to be defined. These matrices define the relevant velocity kinematics and force transmission properties of the contact points. Before the grasp matrix can be defined the definition of a contact is needed. When a contact is located on a rigid body, the configuration m can be defined as a map where the total amount of contact wrenches exerted on a rigid body which depend on the structure of the contact alone can be defined as n_c [60]. This definition can be seen in Equation 5. When a group of contacts are being applied on a rigid body it can be ·at one point (fingertip location). Each contact point defines a map (Equation 7), for $i = \{1,\cdots,k\}$. A map of a

hand with k fingers grasping a rigid body configuration (m) can be represented in Equation 7. The grasping matrix G can be defined (Equation 8).

$$\psi_c = R^{n_c} \rightarrow T_m^* M \tag{6}$$

$$\psi_{ci} = R^{n_i} \rightarrow T_m^* M \tag{7}$$

$$G = R^n \rightarrow T_m^* M,\ n = \sum_{i=1}^{i=k} n_i$$

$$G(x_1, x_2 \cdots, x_n) = \psi_{c1}(x_1, \cdots, x_{ni}) + \cdots + \psi_{ck}(x_{n-n_k,} \cdots, x_n) \tag{8}$$

By referring to Figure 16 a grasp matrix can be produced by using the following procedure: a) Defining an object coordinate and obtaining each contact point coordinate. b) defining the normal and the two orthogonal tangent vectors in relation to the contacting surfaces and points. c) Select an origin of torque in the object body coordinates and define the contact matrix for each contact map. d) Consolidate these contact matrices into a final grasping matrix. Before creating a grasping matrix for the example seen in Figure 16 each finger needs to be defined. Equation 9 defines the first finger map (ψ_{c1}) taking the normal force being applied to the body of wrenches. Equation 10 defines the second finger map (ψ_{c2}) which deals with the finger force and two orthogonal friction forces applied to the body of the wrench. Equation 11 defines the finger 3 map (ψ_{c1}) which accounts for the three applied finger forces and one normal torque to the body of the wrench. By adding the contact maps seen in Equation 9, 10, and 11 the grasp matrix map can be defined for Figure 16 (Equation 12). The calculation of the grasping matrix is crucial for defining

various grasping quality indexes. A benefit of SynGrasp is the system can calculate the grasping matrix of a desired grasping configuration.

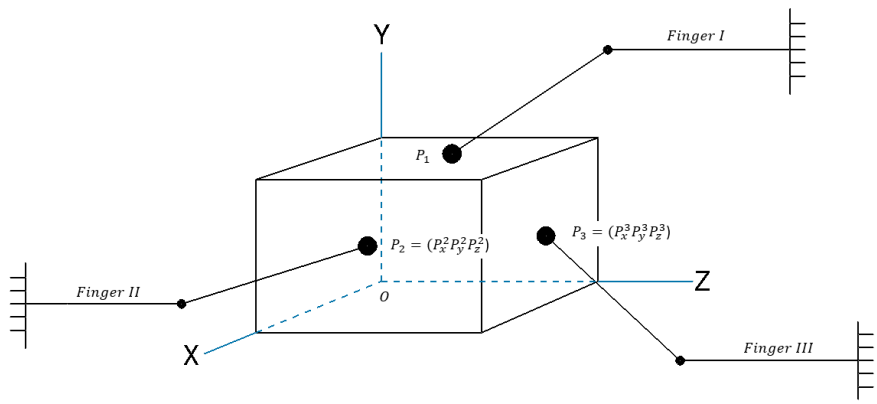

Figure 16: 3-Finger Contact Model Example

$$\psi_{c1} = R^1 \rightarrow T_m^* M$$

$$\psi_{c1}(x) = \begin{bmatrix} f_1^1 \\ f_1^1 \times (p_1 - o) \end{bmatrix}, x = \begin{bmatrix} 0 \\ 0 \\ 1 \\ -p_y^1 \\ p_x^1 \\ 0 \end{bmatrix} \tag{9}$$

$\psi_{c2} = R^3 \rightarrow T_m^* M$

$$\psi_{c2}(x_1, x_2, x_3) = \begin{bmatrix} f_1^2 & f_2^2 & f_3^2 \\ f_1^2 \times (p_2 - o) & f_2^2 \times (p_2 - o) & f_3^2 \times (p_2 - o) \end{bmatrix} \begin{bmatrix} x_1 \\ x_2 \\ x_3 \end{bmatrix}$$

$$= \begin{bmatrix} 1 & 0 & 0 \\ 0 & 1 & 0 \\ 0 & 0 & 1 \\ 0 & p_z^2 & -p_y^2 \\ -p_z^2 & 0 & p_x^2 \\ p_x^2 & -p_x^2 & 0 \end{bmatrix} \begin{bmatrix} x_1 \\ x_2 \\ x_3 \end{bmatrix} \tag{10}$$

$\psi_{c3} = R^4 \rightarrow T_m^* M$

$$\psi_{c3}(x_1, x_2, x_3, x_4) = \begin{bmatrix} f_1^3 & f_2^3 & f_3^3 & 0 \\ f_1^3 \times (p_3 - o) & f_2^3 \times (p_3 - o) & f_3^3 \times (p_3 - o) & m_4^3 \end{bmatrix} \begin{bmatrix} x_1 \\ x_2 \\ x_3 \\ x_4 \end{bmatrix}$$

$$= \begin{bmatrix} 0 & 1 & 0 & 0 \\ 1 & 0 & 0 & 0 \\ 0 & 0 & 1 & 0 \\ p_z^3 & 0 & -p_y^3 & 0 \\ 0 & -p_z^3 & p_x^3 & 1 \\ -p_x^3 & p_x^3 & 0 & 0 \end{bmatrix} \begin{bmatrix} x_1 \\ x_2 \\ x_3 \\ x_4 \end{bmatrix} \tag{11}$$

$$G = \begin{bmatrix} f_1^1 & f_1^2 & f_2^2 & f_3^2 & f_1^3 & f_2^3 & f_3^3 & 0 \\ f_1^1 \times (p_1 - o) & f_1^2 \times (p_2 - o) & f_2^2 \times (p_2 - o) & f_3^2 \times (p_2 - o) & f_1^3 \times (p_3 - o) & f_2^3 \times (p_3 - o) & f_3^3 \times (p_3 - o) & m_4 \end{bmatrix}$$

$$= \begin{bmatrix} 0 & 1 & 0 & 0 & 0 & 1 & 0 & 0 \\ 0 & 0 & 1 & 0 & 1 & 0 & 0 & 0 \\ 1 & 0 & 0 & 1 & 0 & 0 & 1 & 0 \\ -p_y^1 & 0 & p_z^2 & -p_y^2 & p_z^3 & 0 & -p_y^3 & 0 \\ p_x^1 & -p_z^2 & 0 & p_x^2 & 0 & -p_z^3 & p_x^3 & 1 \\ 0 & p_x^2 & -p_x^2 & 0 & -p_x^3 & p_x^3 & 0 & 0 \end{bmatrix} \tag{12}$$

4.3.2 Defining the Jacobian Matrix

When defining the hand Jacobian (J) let $\omega_{i,hnd}^{N}$ represent the angular velocity of the finger/link touching the object contact i [61]. Let $v_{i,hnd}^{N}$ as the translation velocity on the hand in regard to contact i. In both of these representations contact i is expressed as $\{\mathrm{N}\}$. These velocities and the joint velocities are related through the matrix Z_i. Plücker coordinates are used to define the columns of the axes of the joints for matrix Z_i [62, 63]. We have:

$$\begin{pmatrix} v_{i,hnd}^{N} \\ \omega_{i,hnd}^{N} \end{pmatrix} = Z_i \dot{q}, \tag{13}$$

Where $Z_i \in \mathbb{R}^{6\times n_q}$ can be described as:

$$Z_i = \begin{pmatrix} d_{i,1} & \cdots & d_{i,1} \\ l_{i,1} & \cdots & l_{i,n_q} \end{pmatrix}, \tag{14}$$

With the $d_{i,j}, l_{i,j} \in \mathbb{R}^3$defined as:

$$d_{i,j} = \begin{cases} 0_{3\times 1} \\ \hat{\mathrm{z}}_j \\ S(c_i - \zeta_j)^{\intercal}\hat{\mathrm{z}}_j \end{cases} \tag{15}$$

$$l_{i,j} = \begin{cases} 0_{3\times 1} \\ 0_{3\times 1} \\ \hat{\mathrm{z}}_j \end{cases} \tag{16}$$

Where the unit vector in the direction of the z-axis and in the same frame is $\hat{\mathrm{z}}_j$ and the origin of the coordinate frame relating to the j-th joint is ζ_j [61]. In addition, both frames are represented in $\{N\}$.The Denavit-Hartenberg method can be used to assign these frames. The axis that will be used for the rotational axis for the joint revolute and for the translation for prismatic

joint will be the $\hat{z}_j$-axis. The frame of the expression will need to be changed in order to complete the final step in referring the hand twist to the contact frames. The change involves $v_{i,hnd}^N$ and $\omega_{i,hnd}^N$ to $\{C\}_i$:

$$\nu_{i,hnd} = \bar{R}_j^{\intercal} \begin{pmatrix} v_{i,hnd}^N \\ \omega_{i,hnd}^N \end{pmatrix}. \tag{17}$$

The partial hand Jacobian which relates to the joint velocities to the contact twists on the hand can be determined by combining Equation 17 and Equation 13:

$$\nu_{i,hnd} = \tilde{J}_i \dot{q}, \tag{18}$$

Where:

$$\tilde{J}_i = \tilde{J}_i \bar{R}_j^{\intercal} Z_i, \tag{19}$$

By stacking the twist of the hand and the object into the vectors $v_{c,hnd} \in \mathbb{R}^{6n_c}$ and $v_{c,obj} \in \mathbb{R}^{6n_c}$ you get the following compacted notion:

$$v_{c,\xi} = \begin{pmatrix} v_{1,\xi}^{\intercal} & \cdots & v_{n_c,\xi}^{\intercal} \end{pmatrix}, \quad \xi = \{obj, hnd\}. \tag{20}$$

To solve the complete hand Jacobian $\tilde{J} \in \mathbb{R}^{6n_c \times n_q}$ the various velocity quantities as :

$$v_{c,hand} = \tilde{J}\dot{q}, \tag{21}$$

Where:

$$\tilde{J} = \begin{pmatrix} \tilde{J}_1 \\ \vdots \\ \tilde{J}_{n_c} \end{pmatrix} \tag{22}$$

4.3.3 Defining the Grasping Quality Measures

A complete grasp matrix $G \in \mathbb{R}^{6 \times r}$ has 6 singular values given. These values are provided by the positive square roots of the eigenvalues of GG^T [59]. When at least one of the singular values of G goes to zero, the grasp is in a singular configuration. It is beneficial to avoid a singular configuration because the grasp loses the capability of withstanding external wrenches in at least one direction. The quality measurement that indicates how far the grasp is from falling into a singular configuration is known as $\sigma_{min}(G)$ which is the smallest singular value of the grasp matrix G [60]. $\sigma_{min}(G)$ serves as a quality index and is known as the minimum singular value (Q_{MSV}) of G quality measure. A larger $\sigma_{min}(G)$ leads to a better grasp. In addition, a larger $\sigma_{min}(G)$ results in larger minimum contributions from the contact point forces in relation to the net wrench on the object.

Another quality measurement known as the distance to singular configuration is similar to the previously described smallest singular value configuration of G. However, a main difference is the distance to singular configuration considers the object grasping matrix (G) and the hand Jacobian (J). By combining these two properties a physical condition is being added to the quality measure which becomes a critical measurement from a practical point of view. By maximizing the smallest singular value (σ_{min}) of the Jacobian it is possible to keep redundant arms away from reaching a singular configuration [64]. This principle can be applied to hand grasping Jacobian H [59]. The quality index for the distance to singular configuration quality measurement is σ_{min} (H) . The greater the σ_{min} (H) the better the grasp.

In order to consider all singular values H another quality index can be used known as volume of the manipulability ellipsoid [65]. At the fingertips, the forces (f) and velocities (v) are related to the finger joint torques (T) and velocities ($\dot{\theta}$) though the hand Jacobian ($J_h =$

$diag[J_1 \quad \cdots \quad J_i] \epsilon \mathbb{R}^{nr \times nm}$) where $J_i \epsilon \mathbb{R}^{r \times m}, i = 1, \ldots, n$, represents the Jacobian for the finger that is being related to the variables at the finger joint which is also related to the variables at the fingertips:

$$v = J_h \dot{\theta} \tag{23}$$

$$T = J_h^T f \tag{24}$$

The relationship between the forces (f) located on the fingertips, the total wrench (ω) applied on the object, the velocities (v) at the contact points, and the twist ($\dot{x}$) is given by the grasp matrix $G \epsilon \mathbb{R}^{d \times nr}$ [66]:

$$v = G^T \dot{x} \tag{25}$$

$$\omega = Gf \tag{26}$$

Equation 26 is derived by combining Equation 23 and 25:

$$J_h \dot{\theta} = G^T \dot{x} \qquad (26)$$

By utilizing Equation 23 and the velocities at the contact points it is possible to derive the object's velocity. Where $N(G^T)$ represents a matrix where the columns create a basis for the null space of G^T, $(G^T)^+$ denotes the pseudoinverse of G^T, and the arbitrary vector that parametrizes the set solution is represented by v_0. It is important to note that since $G^T \epsilon \mathbb{R}^{nr \times d}$is usually not a square matrix, the pseudoinverse is required. In addition, to create any wrench or twist on the desired object it is necessary that $N(G^T) = 0$ or $rank(G) = d$ [61]. Ultimately, these conditions simplify Equation 28 to $\dot{x} = (G^T)^+ v$ [59]. Via the hand-object Jacobian H, the transformation of the velocity domain starting from the higher dimension joint space to the lower dimensional object space can be accomplished as seen in Equation 29. Where $H = (G^T)^+ J_h \epsilon \mathbb{R}^{d \times nm}$. This

analysis is typically used as more of a dynamic approach and is not typically considered to play a huge role in grasping, however there have been dynamic grasping examples reported [67].

$$\dot{x} = (G^T)^+ v + N(G^T) v_0 \qquad (28)$$

$$\dot{x} = H\dot{\theta} \qquad (29)$$

The volume of the manipulability ellipsoid previously described is mapped utilizing Equation 29 in addition with a sphere of unitary radius in relation to the velocity domain of the finger joints into the object's velocity domain represented by Equation 30. Where $\sigma_1 \sigma_2 \cdots \sigma_r$ represents the singular values of H. A larger quality index signifies that for the similar velocities that reside in the finger joints, a larger velocity of grasped object is being produced. The greater the index the greater the ellipsoid volume measurement more than likely the grasp is better [60].

$$Q_{VME} = \sqrt{\det(HH^T)} = \sigma_1 \sigma_2 \cdots \sigma_r \qquad (30)$$

An important benefit of SynGrasp is the ability to calculate these quality measures of desired grasping configurations. Consider three different grasping configurations. All three configurations will consist of the SynGrasp 3-fingered hand mechanism. In addition, each hand configuration will be grasping a different shaped object which includes a sphere, cube, and cylinder. By calculating the Q_{MSV} quality measure for each grasp it can be determined which grasp is more stable [59, 60, 68]. The greater the Q_{MSV} the better the grasp. Table 1 illustrates each grasp configuration, and it is Q_{MSV} quality measurements. When comparing all the quality indexes it can be stated that the sphere grasping configuration is the best grasp, the cylinder grasping configuration is the second-best grasp, and the cube grasping configuration is the worst of the three grasps. By using this method, the initial grasp in the control algorithm can be analyzed and compared to the second grasp caused by the object perturbance. If the second grasp

has a lower quality per quality measurement, then that can be the signal to begin the impedance algorithm which should re-stabile the grasp causing the quality measurements to improve.

Table 1
Q_{MSV} Grasping Analysis

Grasp Configuration	Quality Index $Q_{MSV} = \sigma_{min}(G)$
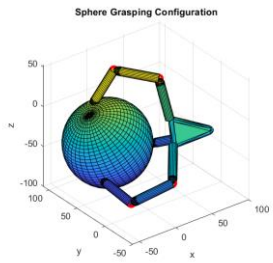	1.710639031520675
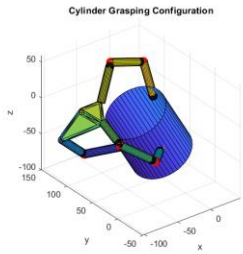	1.694984281515113
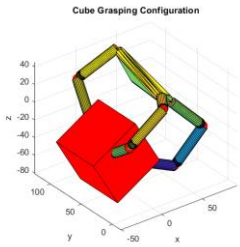	1.620627829845456

4.3.4 Modeling the Perturbed Object and Analyzing the Grasp

There are many degrees of freedom (DoF) distributed among the various kinematic chains known as the fingers in the human hand. In order to mimic the functionality of the human hand a complex mechanical design is needed. Although many roboticists have attempted to mimic the functionality of the human hand in order to match all the hand's DoF, it requires a large amount of actuator motors [69-71]. To combat this issue underactuation designs have been implemented which means essentially the system has more DoF then actuators [72].

Underacuation hands can simplify a control scheme especially in human hands. More specifically studies in neuroscience have demonstrated that input variables known as postural synergies are able to cover most variances in hand motions and grasping configurations [57, 73]. Due to the reduced dimension representation in hand models (compared to biological human hands) synergies or soft synergies can represent joint displacement aggregation. A variation of soft synergy actuation forces can be expressed as:

$$\Delta\sigma = K_z(\Delta z_r - \Delta z) \tag{31}$$

The symmetric and positive definite matrix which is used to define the synergy stiffness is represented by $K_z \in \Re^{n_z \times n_z}$ and the different variation of synergy reference values is represented by Δz_r.

As previously described SynGrasp allows the upload of soft synergy values into the hand modeling to have control on how the mechanism's joints react. The joint displacement is coupled mechanically and in relation to the human hand these synergies are associated to the hand model by a 1 X 20 matrix. By utilizing the initial synergies gathered from the article by Prattichizzo, D., et al, a quality measurement for the first grasp can be calculated [56]. Once the desired values are calculated for the initial grasp, in order to mimic the object perturbance, the hand synergies can be manipulated. This will represent a random object perturbance. Once the synergies are changed a new hand configuration will be created. Quality measurements can then be calculated for the second configuration. The initial and final quality measures will be analyzed to determine if the stabilizing algorithm is necessary.

4.3.5 SynGrasp Implementation of Stabilizing Algorithm

After the object is perturbed and the second grasping configuration is deemed less stable, the stabilization algorithm will need to be incorporated to stabilize the grasp. Since it is known the initial grasp quality is better, in relation to the quality measurement tests, the stabilizing algorithm will need to provide the forces needed to return the second-hand configuration back to the initial hand configuration. SynGrasp can be utilized to provide the unknown variables needed to calculate the finger force needed in Equation 5 and the joint torques needed in Equation 4. The implementation of stabilizing algorithm layout can be seen in Figure 17.

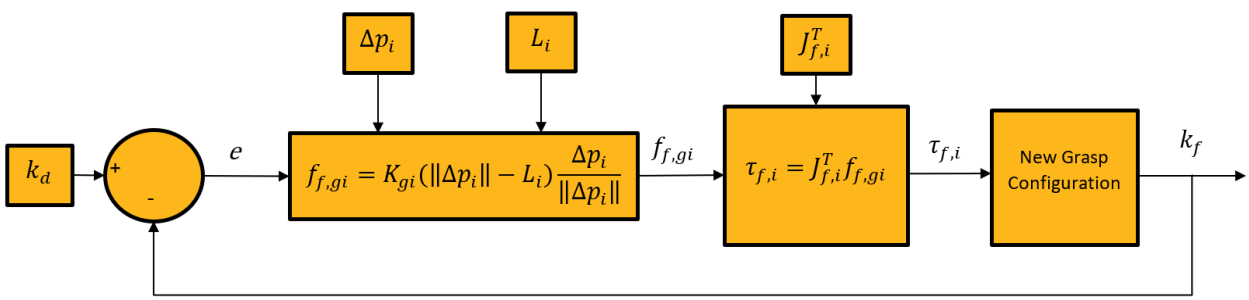

Figure 17: Implementation of Stabilizing Algorithm Layout

Where k_d is the desired stiffness value. This desired stiffness value k_d is the same as K_{gi} which will be incorporated in order to calculate the desired force needed for stabilization ($f_{f,gi}$). Once the force is calculated, the value will be used to find the joint torques ($\tau_{f,i}$) needed for the new hand configuration. k_f is the final stiffness value for the newly calculated hand grasp configuration which will also serve as the feedback loop which will help minimize the error e ($e = k_f - k_d$) in order to ensure the final stiffness is as close as possible to the desired stiffness.

Once the hand is being modeled and the object in the grasping pattern is being created by using the function *SGmakeObject(hand)*, the MATLAB workspace will create an object structure file. Within this object structure file, you can derive the calculated object center as well as the contact points on the object for each finger. The contact points are represented by a 4 X 3 matrix for a 3-fingered contact model and the object center represented by a 1 X 3 matrix. With this information Δp_i can be calculated. In addition, since the soft synergies will be incorporated to the hand model then the stiffness K_{gi} can be calculated. The synergies can be seen in the workspace, it is referred to as the qm file which is represented by a 1 X 20 matrix. Since L_i is the desired distance from each finger to the object frame that distance can be calculated with the contact points and object center location. The desired L_i will need to be calculated from the initial grasping configuration since it is considered the more stable grasp configuration at this point of the control method. When all these variables are incorporated into Equation 5 then $f_{f,gi}$ can be solved.

CHAPTER 5

EXPERIMENT AND RESULTS

5.1 Impedance Control Algorithm

To create a grasping configuration that closely mimics the human hand the SGparadigmatic was uploaded from the SynGrasp library. The SynGrasp library has already pre-defined the DH parameters needed to create a 5-fingered hand model (Table 2). The function SGsantelloSynergies will be utilized to apply the soft synergies needed to define the joint stiffnesses that mimic human hand joint stiffnesses. Figure 18 numbers the joint that will be affected by the synergies. The synergy matrix file qm defines the synergies with a 1 X 20 matrix. However, since the grasping configuration that is going to be analyzed is a 3-fingered configuration only the first 12 matrix positions will be considered since they affect the 3 fingers being used in the grasping configuration. Equation 31 will notate what matrix position affects what finger.

Table 2
Finger DH Parameter Definitions

Finger Modeling Parameters						
	Thumb	Index	Middle	Ring	Little	Joint Being Affected
DHpars{} DH Parameters	$\begin{bmatrix} \frac{-\pi}{2} & 0 & 0 & 0 \\ 0 & 25 & 0 & 0 \\ \frac{\pi}{2} & 15 & 0 & 0 \\ 0 & 10 & 0 & 0 \end{bmatrix}$	$\begin{bmatrix} \frac{-\pi}{2} & 0 & 0 & 0 \\ 0 & 37 & 0 & 0 \\ 0 & 30 & 0 & 0 \\ 0 & 15 & 0 & 0 \end{bmatrix}$	$\begin{bmatrix} \frac{-\pi}{2} & 0 & 0 & 0 \\ 0 & 40 & 0 & 0 \\ 0 & 35 & 0 & 0 \\ 0 & 17 & 0 & 0 \end{bmatrix}$	$\begin{bmatrix} \frac{-\pi}{2} & 0 & 0 & 0 \\ 0 & 37 & 0 & 0 \\ 0 & 30 & 0 & 0 \\ 0 & 15 & 0 & 0 \end{bmatrix}$	$\begin{bmatrix} \frac{-\pi}{2} & 0 & 0 & 0 \\ 0 & 37 & 0 & 0 \\ 0 & 30 & 0 & 0 \\ 0 & 15 & 0 & 0 \end{bmatrix}$	$\begin{bmatrix} MCP\ abd/add \\ MCP\ flex/ext \\ PIP\ felx/ext \\ DIP\ flex/ext \end{bmatrix}$ *does not include thumb
base{}	$\begin{bmatrix} 0 & -1 & 0 & -37 \\ 1 & 0 & 0 & 45 \\ 0 & 0 & 1 & 0 \\ 0 & 0 & 0 & 1 \end{bmatrix}$	$\begin{bmatrix} 0 & -1 & 0 & -24 \\ 1 & 0 & 0 & 73 \\ 0 & 0 & 1 & 0 \\ 0 & 0 & 0 & 1 \end{bmatrix}$	$\begin{bmatrix} 0 & -1 & 0 & -8 \\ 1 & 0 & 0 & 73 \\ 0 & 0 & 1 & 0 \\ 0 & 0 & 0 & 1 \end{bmatrix}$	$\begin{bmatrix} 0 & -1 & 0 & 8 \\ 1 & 0 & 0 & 73 \\ 0 & 0 & 1 & 0 \\ 0 & 0 & 0 & 1 \end{bmatrix}$	$\begin{bmatrix} 0 & -1 & 0 & 24 \\ 1 & 0 & 0 & 73 \\ 0 & 0 & 1 & 0 \\ 0 & 0 & 0 & 1 \end{bmatrix}$	

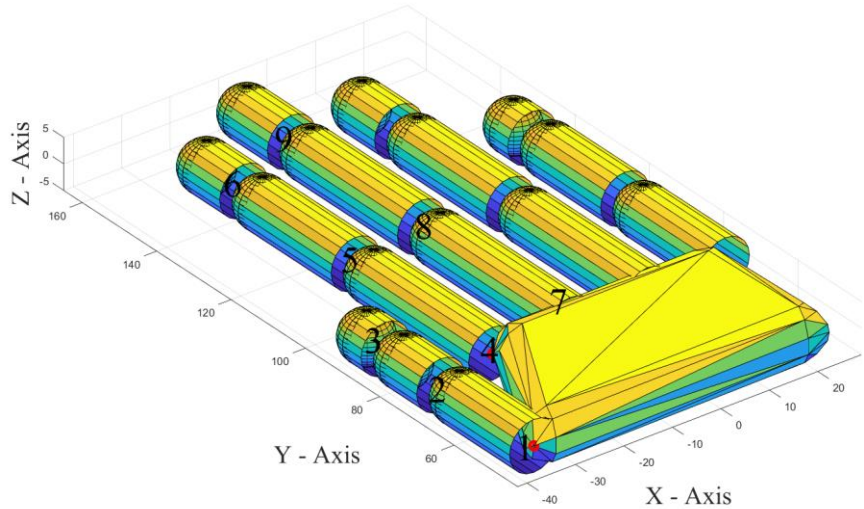

Figure 18: 5-Fingered Hand Joint Numbering

$$qm = \begin{bmatrix} j_{1,z} \\ j_{1,x} \\ j_{2,x} \\ j_{3,z} \\ j_{4,z} \\ j_{4,x} \\ j_{5,x} \\ j_{6,x} \\ j_{7,z} \\ j_{7,x} \\ j_{8,x} \\ j_{9,x} \end{bmatrix} \begin{matrix} Affects\ joint\ 1\ about\ the\ z\ axis \\ Affects\ joint\ 1\ about\ the\ x\ axis \\ Affects\ joint\ 2\ about\ the\ x\ axis \\ Affects\ joint\ 3\ about\ the\ z\ axis \\ Affects\ joint\ 4\ about\ the\ z\ axis \\ Affects\ joint\ 4\ about\ the\ x\ axis \\ Affects\ joint\ 5\ about\ the\ x\ axis \\ Affects\ joint\ 6\ about\ the\ x\ axis \\ Affects\ joint\ 7\ about\ the\ z\ axis \\ Affects\ joint\ 7\ about\ the\ x\ axis \\ Affects\ joint\ 8\ about\ the\ x\ axis \\ Affects\ joint\ 9\ about\ the\ x\ axis \end{matrix} \tag{31}$$

By utilizing the function *SGaddFtipContact(),* the contact points can be located on the fingertips. For this experiment only the thumb, index, and middle finger will be considered into the grasping configuration. The function SGmakeObject(hand) allows the object to be plotted based on the fingertip contact point locations. Figure 19 will show the initial grasp plot which included the SGparadigmatic hand with synergies incorporated as well as the object. In addition,

the output data which is seen in the workspace will have information like the synergy definition matrix (qm), hand structure information (which contains the hand Jacobean (J)), and the object structure information (which contains the object center, contact points, and grasping matrix (G)).

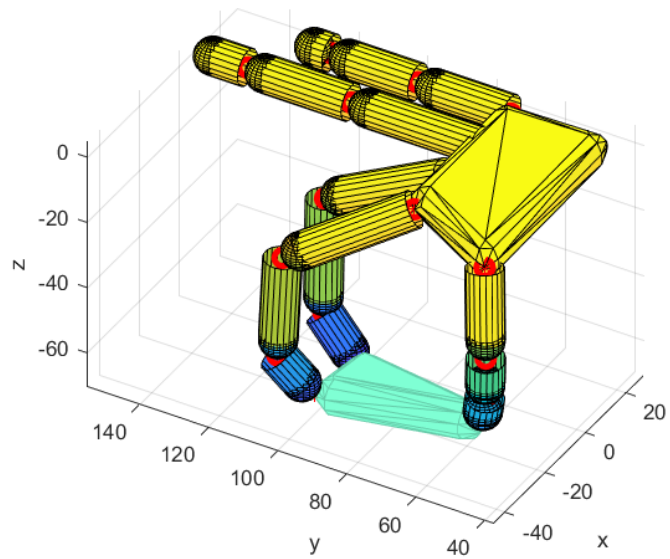

Figure 19. Initial Grasping Configuration

Once the initial grasp has been fully defined the function *SGmanipEllipsoidVolume()* was used to calculate the volume of the manipulability ellipsoid quality measurement. In addition, the function *SGdistSingularConfiguration()* was used to calculate the distance to singular configuration quality measurement. Both of these functions use the hand Jacobian and grasping matrix as inputs. The output index values can be seen in the MATLAB workspace. Once the initial grasp analysis has been complete the object perturbance is incorporated. To model the grasped object being perturbed the initial synergies (qm) are changed randomly in order to mimic a random object perturbation. The new (final) grasping configuration can be seen in Figure

20.The differences between the initial grasp synergies, grasp matrix, hand Jacobean, and the quality measurements can be seen in Table 3-6. By analyzing the quality measures the estimation function of the proposed algorithm can conclude that the final grasp is unstable due to the fact that the indexes for the initial grasp are higher for both the volume of the manipulability ellipsoid and singular configuration quality measurement. Thus, the stability algorithm would need to be activated to re-stabilize the grasp configuration. When initiating the impedance control algorithm various variables need to be calculated in order to solve Equation 4 and Equation 5. These missing variables can be found by using SynGrasp as an analyzing tool of the proposed grasp object dynamic model. It is important that the desired variables are gathered form the correct hand configurations. k_d and L_i will be collected from the initial grasp the stability needs to be mimicked. Δp_i will be gathered from the final grasp configuration since it is the grasp which will be modified to create the new configuration.

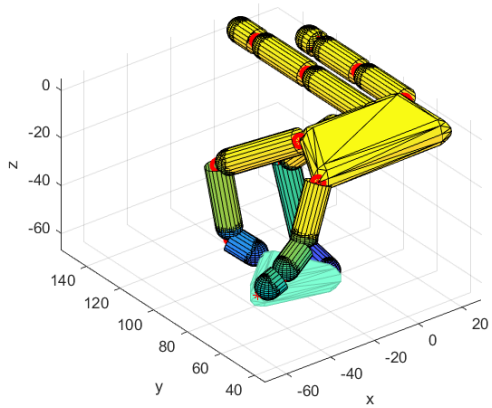

Figure 20: Final Grasp Configuration

Table 3
Synergy Matrix Comparison

	Synergy Matrix (qm)
Initial Grasp	$\begin{bmatrix} -0.983 \\ 1.760 \\ -0.430 \\ 0.092 \\ 0.453 \\ 0.467 \\ 1.060 \\ 0.707 \\ 0 \\ 0.495 \\ 1.060 \\ 0.707 \end{bmatrix}$
Final Grasp	$\begin{bmatrix} -1.30 \\ 2.00 \\ 0.70 \\ 0.30 \\ 0.50 \\ 0.50 \\ 1.25 \\ 1.00 \\ 0 \\ 0.75 \\ 1.20 \\ 1 \end{bmatrix}$

Table 4
Grasp Matrix Comparison

	Grasp Matrix (G)
Initial Grasp	$\begin{bmatrix} 1 & 0 & 0 & 1 & 0 & 0 & 1 & 0 & 0 \\ 0 & 1 & 0 & 0 & 1 & 0 & 0 & 1 & 0 \\ 0 & 0 & 1 & 0 & 0 & 1 & 0 & 0 & 1 \\ 0 & -9.32 & -33.52 & 0 & 0.33 & 15.63 & 0 & 8.99 & 17.90 \\ 9.32 & 0 & 9.95 & -0.33 & 0 & 8.53 & -8.99 & 0 & -18.49 \\ 33.52 & -9.95 & 0 & -15.62 & -8.53 & 0 & -17.90 & 18.49 & 0 \end{bmatrix}$
Final Grasp	$\begin{bmatrix} 1 & 0 & 0 & 1 & 0 & 0 & 1 & 0 & 0 \\ 0 & 1 & 0 & 0 & 1 & 0 & 0 & 1 & 0 \\ 0 & 0 & 1 & 0 & 0 & 1 & 0 & 0 & 1 \\ 0 & -16.51 & -26.33 & 0 & 3.24 & 19.17 & 0 & 13.27 & 7.16 \\ 16.52 & 0 & 33.35 & -3.24 & 0 & -5.50 & -13.27 & 0 & -27.85 \\ 26.33 & -33.35 & 0 & -19.17 & 5.50 & 0 & -7.16 & 27.85 & 0 \end{bmatrix}$

Table 5
Hand Jacobean Matrix Comparison

	Hand Jacobean (J)
Initial Grasp	$\begin{bmatrix} -1.47 & -40.59 & -20.16 & -5.71 & 0 & 0 & 0 & 0 & 0 & 0 & 0 & 0 \\ 0.56 & -27.07 & -13.45 & 8.16 & 0 & 0 & 0 & 0 & 0 & 0 & 0 & 0 \\ 0 & -1.28 & -5.97 & 0.89 & 0 & 0 & 0 & 0 & 0 & 0 & 0 & 0 \\ 0 & 0 & 0 & 0 & -22.62 & 25.60 & 18.31 & 5.18 & 0 & 0 & 0 & 0 \\ 0 & 0 & 0 & 0 & -11.02 & -52.54 & -37.58 & -10.64 & 0 & 0 & 0 & 0 \\ 0 & 0 & 0 & 0 & 0 & -25.16 & 7.89 & 9.22 & 0 & 0 & 0 & 0 \\ 0 & 0 & 0 & 0 & 0 & 0 & 0 & 0 & -24.89 & -1.52e^{-15} & 6.31e^{-16} & 6.64e^{16} \\ 0 & 0 & 0 & 0 & 0 & 0 & 0 & 0 & -355e^{-15} & -67.12 & -48.09 & -13.10 \\ 0 & 0 & 0 & 0 & 0 & 0 & 0 & 0 & 0 & -24.89 & 10.30 & 10.84 \end{bmatrix}$
Final Grasp	$\begin{bmatrix} 5.87 & -32.02 & -10.11 & 0.02 & 0 & 0 & 0 & 0 & 0 & 0 & 0 & 0 \\ -32.20 & -8.89 & -2.81 & 9.92 & 0 & 0 & 0 & 0 & 0 & 0 & 0 & 0 \\ 0 & 32.60 & 22.20 & 1.26 & 0 & 0 & 0 & 0 & 0 & 0 & 0 & 0 \\ 0 & 0 & 0 & 0 & -11.64 & 25.40 & 16.90 & 2.74 & 0 & 0 & 0 & 0 \\ 0 & 0 & 0 & 0 & -6.36 & -46.50 & -30.93 & -5.02 & 0 & 0 & 0 & 0 \\ 0 & 0 & 0 & 0 & 0 & -13.26 & 19.21 & 13.86 & 0 & 0 & 0 & 0 \\ 0 & 0 & 0 & 0 & 0 & 0 & 0 & 0 & 0.38 & 2.31e^{-17} & 1.82e^{-15} & 1.02e^{-15} \\ 0 & 0 & 0 & 0 & 0 & 0 & 0 & 0 & -355e^{-15} & -63.02 & -35.75 & -3.24 \\ 0 & 0 & 0 & 0 & 0 & 0 & 0 & 0 & 0 & 0.38 & 29.65 & 16.69 \end{bmatrix}$

Table 6
Quality Measurement Comparison

	Manipulability Ellipsoid VE	Singular Configuration SminHO
Initial Grasp	$3.2357e^{03}$	0.3425
Final Grasp	770.72	0.0975

Table 7
Desired Variables for Force Calculation

Desired Variables	
$k_d = K_{gi}$	$\begin{bmatrix} 0.02 & -5.69e^{-04} & .001 & -0.02 & -0.17 & -0.15 \\ -5.70e^{-04} & 0.007 & -9.41e^{-04} & -0.03 & -0.04 & -0.18 \\ 0.001 & -9.41e^{-04} & 0.01 & -0.22 & 0.17 & 0.06 \\ -0.02 & -0.03 & -0.22 & 7.35 & -4.96 & 0.13 \\ -0.17 & -0.04 & 0.17 & -4.96 & 7.57 & 3.91 \\ -0.15 & -0.18 & 0.06 & 0.13 & 3.91 & 7.30 \end{bmatrix}$
p_o	$\begin{bmatrix} -27.60 \\ 70.35 \\ -54.22 \end{bmatrix}$
p_i=1,2,3	$\begin{bmatrix} -36.441 & -35.019 & -8.000 \\ 46.4724233005936 & 95.6174864330797 & 97.889 \\ -48.789 & -58.444 & -67.107 \\ 1 & 1 & 1 \end{bmatrix}$
L_i=1,2,3	$L_1 = 125.85; L_2 = 172.93, L_3 = 140.51$

5.2 Discussion of Potential Future Work

The next step after the algorithm has been defined is to apply the proposed control system to a physical robotic hand. More specifically a prosthetic hand since the ultimate goal is to improve prosthesis functionality. There have been studies conducted involving SynGrasp interfacing with real time robotics [54, 55]. By implementing the control system to a real time prosthetic hand more data can be collected which can be used to see the effectiveness of the proposed control system.

In addition, by updating the adaptation method to incorporate myoelectric control in a prosthetic upper limb, a user to mechanism interface regarding prosthetic control can be significantly improved. Although recent advances in prosthetic control developments have seen an explosion of innovation, there is still a lag pertaining to the user's ability to control the functionality of the prosthetic mechanism. Various studies have shown that by incorporating haptic feedback from a prosthetic, leads to performance improvements in certain tasks [74-76]. For example, the article by Meek, S.G., et al, showed that by incorporating a pressure cue and delivering it to the prosthetic limb the user was able to maintain a grip force more efficiently which significantly decreased slippage situations [77]. Similarly, in this study the impedance control method so far described above can be utilized to determine if a grasp is unstable or not. If the grasp is unstable a haptic feedback will be provided to the user providing a signal that the grasp is unstable which then the user can then provide more force using myoelectric signals. The force increased in each finger, which is needed to restabilize the grasp, is instead produced by the user and not automatic like various impedance control methods use.

CHAPTER 6

CONCLUSIONS AND RECOMMENDATION

In this thesis an adaptive impedance control system was proposed. The control system included various sections. These sections include the initial grasp, stability estimation function, and the impedance adaptation section. Although impedance control systems are not a new concept this thesis proposed a unique way to tackle the stability estimation function by utilizing grasping quality measures. These quality measures are calculated by using properties of the grasping configuration. In addition, this thesis introduced how to utilize a MATLAB toolbox in order to simulate the proposed impedance control system. SynGrasp allows the design and analysis of the grasp configurations being studied. Although there were issues with figuring out how to simulate a grasped object being perturbed, this issue was solved by changing the model hand synergies.

Although SynGrasp is capable of simulating the proposed estimation function and it has the capabilities to provide the information and data needed it still lacked the ability to fully simulate the impedance adaptation portion. However, the study was able to prove that by utilizing grasping quality measures a unique estimation function that revolves around grasping stability can be created. By continuing the research and collecting data by implementing the proposed algorithm in a real time prosthetic hand. It can significantly improve the dexterity of current prosthetic hands. In addition, by incorporating a method where the patient can provide biological signals to personally control the impedance adaptation portion of the proposed control system a more advanced prosthetic that is closer to mimicking the dexterity of the human hand can be created. Improving the science of prosthetic engineering.

REFERENCES

REFERENCES

1. Armour, B.S., et al., Prevalence and Causes of Paralysis-United States, 2013. Am J Public Health, 2016. 106(10): p. 1855-7.

2. Ziegler-Graham, K., et al., Estimating the Prevalence of Limb Loss in the United States: 2005 to 2050. Archives of Physical Medicine and Rehabilitation, 2008. 89(3): p. 422-429.

3. Massa, B., et al. Design and development of an underactuated prosthetic hand. in Proceedings 2002 IEEE International Conference on Robotics and Automation (Cat. No.02CH37292). 2002.

4. Laliberté, T. and C.M. Gosselin, Simulation and design of underactuated mechanical hands. Mechanism and Machine Theory, 1998. 33(1): p. 39-57.

5. Keneko, M., et al. Analysis on detaching assist motion (DAM). in Proceedings 2001 ICRA. IEEE International Conference on Robotics and Automation (Cat. No.01CH37164). 2001.

6. Carrozza, M.C., et al. The development of a novel biomechatronic hand-ongoing research and preliminary results. in 2001 IEEE/ASME International Conference on Advanced Intelligent Mechatronics. Proceedings (Cat. No.01TH8556). 2001.

7. bebionic hand. 2019; Available from: https://www.ottobockus.com/prosthetics/upper-limb-prosthetics/solution-overview/bebionic-hand/.

8. i-Limb Quantum. [Online] 2019; Available from: https://www.ossur.com/prosthetic-solutions/products/touch-solutions/i-limb-quantum.

9. Tack, P., et al., 3D-printing techniques in a medical setting: a systematic literature review. BioMedical Engineering OnLine, 2016. 15(1): p. 115.

10. Carbone, G., Stiffness Analysis for Grasping Tasks, in Grasping in Robotics, G. Carbone, Editor. 2013, Springer London: London. p. 17-55.

11. Duffy, J., Statics and Kinematics with Applications to Robotics. 1996, Cambridge: Cambridge University Press.

12. Sangveraphunsiri, V. and K. Chooprasird, Dynamics and control of a 5-DOF manipulator based on an H-4 parallel mechanism. The International Journal of Advanced Manufacturing Technology, 2011. 52(1): p. 343-364.

13. Sung Kim, H. and H. Lipkin, Stiffness of Parallel Manipulators With Serially Connected Legs. Journal of Mechanisms and Robotics, 2014. 6(3): p. 031001-031001-9.

14. Rivin, E.I. Stiffness and damping in mechanical design. 1999; Available from: http://www.crcnetbase.com/isbn/9780824717223.

15. Hogan, N., Impedance Control: An Approach to Manipulation: Part II—Implementation. Journal of Dynamic Systems, Measurement, and Control, 1985. 107(1): p. 8-16.

16. Kronander, K. and A. Billard, Stability Considerations for Variable Impedance Control. IEEE Transactions on Robotics, 2016. 32(5): p. 1298-1305.

17. Buchli, J., et al., Learning variable impedance control. The International Journal of Robotics Research, 2011. 30(7): p. 820-833.

18. Calinon, S., I. Sardellitti, and D.G. Caldwell. Learning-based control strategy for safe human-robot interaction exploiting task and robot redundancies. in 2010 IEEE/RSJ International Conference on Intelligent Robots and Systems. 2010.

19. Pistillo, A., S. Calinon, and D. G. Caldwell, Bilateral physical interaction with a robot manipulator through a weighted combination of flow fields. 2011. 3047-3052.

20. Gertz, M.W., K. Jin-Oh, and P.K. Khosla. Exploiting redundancy to reduce impact force. in Proceedings IROS '91:IEEE/RSJ International Workshop on Intelligent Robots and Systems '91. 1991.

21. Sigaud, O. and J. Peters, From Motor Learning to Interaction Learning in Robots, in From Motor Learning to Interaction Learning in Robots, O. Sigaud and J. Peters, Editors. 2010, Springer Berlin Heidelberg: Berlin, Heidelberg. p. 1-12.

22. Kronander, Klas, and Aude Billard. "Online learning of varying stiffness through physical human-robot interaction." 2012 IEEE International Conference on Robotics and Automation. Ieee, 2012.

23. Rozo, L., P. Jimenez, and C. Torras. Robot learning from demonstration of force-based tasks with multiple solution trajectories. in 2011 15th International Conference on Advanced Robotics (ICAR). 2011.

24. Kormushev, P., S. Calinon, and D. G. Caldwell, Imitation Learning of Positional and Force Skills Demonstrated via Kinesthetic Teaching and Haptic Input. Vol. 25. 2011.

25. Franklin, D., et al., Adaptation to Stable and Unstable Dynamics Achieved by Combined Impedance Control and Inverse Dynamics Model. Vol. 90. 2003. 3270-82.

26. L Gribble, P., et al., Role of Cocontraction in Arm Movement Accuracy. Vol. 89. 2003. 2396-405.

27. Fukuda, O., et al., A human-assisting manipulator teleoperated by EMG signals and arm motions. IEEE Transactions on Robotics and Automation, 2003. 19(2): p. 210-222.

28. Gomi, H. and M. Kawato, Equilibrium-Point Control Hypothesis Examined by Measured Arm Stiffness During Multijoint Movement. Vol. 272. 1996. 117-20.

29. Burdet, E., et al., The central nervous system stabilizes unstable dynamics by learning optimal impedance. Nature, 2001. 414(6862): p. 446-449.

30. Ganesh, G., et al. Biomimetic motor behavior for simultaneous adaptation of force, impedance and trajectory in interaction tasks. in 2010 IEEE International Conference on Robotics and Automation. 2010.

31. Howard, M., D.J. Braun, and S. Vijayakumar, Transferring Human Impedance Behavior to Heterogeneous Variable Impedance Actuators. IEEE Transactions on Robotics, 2013. 29(4): p. 847-862.

32. Hogan, N., Adaptive control of mechanical impedance by coactivation of antagonist muscles. IEEE Transactions on Automatic Control, 1984. 29(8): p. 681-690.

33. Chen, H. and Y. Liu, Robotic assembly automation using robust compliant control. Robotics and Computer-Integrated Manufacturing, 2013. 29(2): p. 293-300.

34. Rizk, R., S. Krut, and E. Dombre. Grasp-stability analysis of a two-phalanx isotropic underactuated finger. in 2007 IEEE/RSJ International Conference on Intelligent Robots and Systems. 2007.

35. Pozzi, M., M. Malvezzi, and D. Prattichizzo, On Grasp Quality Measures: Grasp Robustness and Contact Force Distribution in Underactuated and Compliant Robotic Hands. IEEE Robotics and Automation Letters, 2017. 2(1): p. 329-336.

36. Tahara, K., S. Arimoto, and M. Yoshida. Dynamic object manipulation using a virtual frame by a triple soft-fingered robotic hand. in 2010 IEEE International Conference on Robotics and Automation. 2010.

37. Tahara, K., et al. Externally sensorless dynamic regrasping and manipulation by a triple-fingered robotic hand with torsional fingertip joints. in 2012 IEEE International Conference on Robotics and Automation. 2012.

38. Li, M., et al. Learning object-level impedance control for robust grasping and dexterous manipulation. in 2014 IEEE International Conference on Robotics and Automation (ICRA). 2014.

39. Nguyen, K. and V. Perdereau. Fingertip force control based on max torque adjustment for dexterous manipulation of an anthropomorphic hand. in 2013 IEEE/RSJ International Conference on Intelligent Robots and Systems. 2013.

40. Wimbock, T., C. Ott, and G. Hirzinger. Analysis and experimental evaluation of the Intrinsically Passive Controller (IPC) for multifingered hands. in 2008 IEEE International Conference on Robotics and Automation. 2008.

41. Bohg, J. and D. Kragic, Learning grasping points with shape context. Robotics and Autonomous Systems, 2010. 58(4): p. 362-377.

42. Rasolzadeh, B., et al., An Active Vision System for Detecting, Fixating and Manipulating Objects in the Real World. The International Journal of Robotics Research, 2009. 29(2-3): p. 133-154.

43. Dang, H. and P.K. Allen, Stable grasping under pose uncertainty using tactile feedback. Autonomous Robots, 2014. 36(4): p. 309-330.

44. Bekiroglu, Y., et al., Assessing Grasp Stability Based on Learning and Haptic Data. IEEE Transactions on Robotics, 2011. 27(3): p. 616-629.

45. Yussof, H., et al. Determination of object stiffness control parameters in robot manipulation using a prototype optical three-axis tactile sensor. in SENSORS, 2008 IEEE. 2008.

46. Zhang, Y., Y. Mukaibo, and T. Maeno. A Multi-Purpose Tactile Sensor Inspired by Human Finger for Texture and Tissue Stiffness Detection. in 2006 IEEE International Conference on Robotics and Biomimetics. 2006.

47. Dahiya, R.S., et al., Tactile Sensing—From Humans to Humanoids. IEEE Transactions on Robotics, 2010. 26(1): p. 1-20.

48. Andrecioli, R. and E.D. Engeberg. Grasped object stiffness detection for adaptive PID sliding mode position control of a prosthetic hand. in 2012 4th IEEE RAS & EMBS International Conference on Biomedical Robotics and Biomechatronics (BioRob). 2012.

49. Andrecioli, R. and E.D. Engeberg. Grasped object stiffness detection for adaptive force control of a prosthetic hand. in 2010 3rd IEEE RAS & EMBS International Conference on Biomedical Robotics and Biomechatronics. 2010.

50. Sundaralingam, B. and T. Hermans, Relaxed-rigidity constraints: kinematic trajectory optimization and collision avoidance for in-grasp manipulation. Autonomous Robots, 2019. 43(2): p. 469-483.

51. Bohg, J., et al., Data-Driven Grasp Synthesis—A Survey. IEEE Transactions on Robotics, 2014. 30(2): p. 289-309.

52. Song, H., M.Y. Wang, and K. Hang, Fingertip Surface Optimization for Robust Grasping on Contact Primitives. IEEE Robotics and Automation Letters, 2018. 3(2): p. 742-749.

53. Boutselis, G.I., et al. Task specific robust grasping for multifingered robot hands. in 2014 IEEE/RSJ International Conference on Intelligent Robots and Systems. 2014.

54. Malvezzi, M., et al., SynGrasp: A MATLAB Toolbox for Underactuated and Compliant Hands. IEEE Robotics & Automation Magazine, 2015. 22(4): p. 52-68.

55. Malvezzi, M., et al. SynGrasp: A MATLAB toolbox for grasp analysis of human and robotic hands. in 2013 IEEE International Conference on Robotics and Automation. 2013.

56. Prattichizzo, D., et al., On Motion and Force Controllability of Precision Grasps with Hands Actuated by Soft Synergies. IEEE Transactions on Robotics, 2013. 29(6): p. 1440-1456.

57. Santello, M., M. Flanders, and J.F. Soechting, Postural hand synergies for tool use. J Neurosci, 1998. 18(23): p. 10105-15.

58. Prattichizzo, D. and J.C. Trinkle, Grasping 28. Grasping. 2016.

59. Roa, M.A. and R. Suárez, Grasp quality measures: review and performance. Autonomous Robots, 2015. 38(1): p. 65-88.

60. Li, Z. and S.S. Sastry, Task-oriented optimal grasping by multifingered robot hands. IEEE Journal on Robotics and Automation, 1988. 4(1): p. 32-44.

61. Prattichizzo, D., et al., Springer handbook of robotics. Grasping; Springer: Berlin/Heidelberg, Germany, 2008: p. 671-700.

62. Ohwovoriole, M.S. and B. Roth, An Extension of Screw Theory. Journal of Mechanical Design, 1981. 103(4): p. 725-735.

63. Hunt, K.H., Kinematic geometry of mechanisms. 1978, Oxford; New York: Clarendon Press ; Oxford University Press.

64. Klein, C.A. and B.E. Blaho, Dexterity Measures for the Design and Control of Kinematically Redundant Manipulators. The International Journal of Robotics Research, 1987. 6(2): p. 72-83.

65. Yoshikawa, T., Manipulability of Robotic Mechanisms. The International Journal of Robotics Research, 1985. 4(2): p. 3-9.

66. Murray, R.M., et al., A mathematical introduction to robotic manipulation. 1994: CRC press.

67. Senoo, T., et al. Skillful manipulation based on high-speed sensory-motor fusion. in 2009 IEEE International Conference on Robotics and Automation. 2009.

68. León, B., et al., Evaluation of Human Prehension Using Grasp Quality Measures. International Journal of Advanced Robotic Systems, 2012. 9(4): p. 112.

69. Jacobsen, S.C., et al., The UTAH/M.I.T. Dextrous Hand: Work in Progress. The International Journal of Robotics Research, 1984. 3(4): p. 21-50.

70. Butterfass, J., et al. DLR-Hand II: next generation of a dextrous robot hand. in Proceedings 2001 ICRA. IEEE International Conference on Robotics and Automation (Cat. No.01CH37164). 2001.

71. Loucks, C., et al. Modeling and control of the stanford/JPL hand. in Proceedings. 1987 IEEE International Conference on Robotics and Automation. 1987.

72. Birglen, L. and C.M. Gosselin, Grasp-state plane analysis of two-phalanx underactuated fingers. Mechanism and Machine Theory, 2006. 41(7): p. 807-822.

73. Santello, M. and J.F. Soechting, Force synergies for multifingered grasping. Exp Brain Res, 2000. 133(4): p. 457-67.

74. Panarese, A., et al., Humans Can Integrate Force Feedback to Toes in Their Sensorimotor Control of a Robotic Hand. Neural Systems and Rehabilitation Engineering, IEEE Transactions on, 2010. 17: p. 560-567.

75. Rombokas, E., et al., Vibrotactile Sensory Substitution for Electromyographic Control of Object Manipulation. IEEE transactions on bio-medical engineering, 2013. 60.

76. Gillespie, R.B., et al., Toward improved sensorimotor integration and learning using upper-limb prosthetic devices. Annu Int Conf IEEE Eng Med Biol Soc, 2010. 2010: p. 5077-80.